Filtering sparse data with 3D tensorial structuring elements

MARCELO B. VIEIRA[1,2], MATTHIEU CORD[2], PAULO P. MARTINS JR.[3],
ARNALDO DE A. ARAÚJO[1], SYLVIE PHILIPP-FOLIGUET[2]

[1]NPDI/DCC - Universidade Federal de Minas Gerais, Caixa Postal 702, 30161-970, Belo Horizonte, MG, Brazil
{bernard,arnaldo}@dcc.ufmg.br
[2]Ecole Nationale Supérieure d'Electronique et de ses Applications, 6 av. du Ponceau, 95014, Cergy Cedex, France
{cord,philipp}@ensea.fr
[3]Centro Tecnológico de Minas Gerais, av. José Cândido da Silveira, 2000, 31170-000, Belo Horizonte, MG, Brazil
pmartin@cetec.br

Abstract. We address in this paper the problem of filtering three-dimensional sparse data representing real objects. The main application is to eliminate points that are not structured on surfaces. Points classified as organized can be the input for other processes. An accumulation process infers the organization of each input element. The tensorial fields used in our method act as three-dimensional structuring elements. They define normal orientations in space indicating possible surface continuations.

1 Introduction

Surface reconstruction is used for the problem of retrieving three-dimensional shapes which, in general, represent a physical object. In most cases, only points distributed over the object are known. Obtaining precise 3D models of real objects has applications in reverse engineering, shape analysis, computer graphics, computer vision, among others.

The most important works on surface reconstruction classify sparse data as an *unorganized point set* [1, 2]. Since the points are organized over an object, we classify them as organized. Their spatial organization effectively allows the extraction of the original structuring object. In fact, reconstruction becomes a problem when information about the points organization is limited or missing.

In Gopi & Krishman [3], a set of points is *organized* if it has additional information about original surface. In our work, organized points are those that, within their neighborhood, are structured over a surface.

Sparse data representing objects may have outliers and additive noise in real applications. In Gideon Guy's paradigm [4, 5], surface reconstruction is made by evaluating the sparse data organization. More precisely, Guy provides two functions $n(D, Q) \rightarrow \mathbb{R}^3$ and $s(D, Q) \rightarrow \mathbb{R}^+$, where D is a sparse data set and $Q \in \mathbb{R}^3$ is an arbitrary point, in such a way that

- $n(D, Q)$ is the estimation of a normal in Q representing a surface that presumably structures Q in conjunction with its neighborhood in D;

- $s(D, Q)$ is the pertinence, or relevance degree of the normal estimate in comparison with the original object represented by D.

Recently, we proposed new mathematical foundations to enhance the sparse data organization inference [6]. The more precise pertinence values provided by our functions may be used to classify each given point as structured or not. In this paper, we propose a method for sparse data filtering suitable for pre-processing purposes.

2 Accumulation method for finding normals

In the method described in [6], the procedures and mathematical notions originally proposed by Guy are adapted for robust normal inference.

More precisely, we propose new tensorial fields that are treated as surface specific *structuring elements* in an accumulation method. These fields are composed by symetric second order *orientation tensors* [7]

$$\boldsymbol{T} = \lambda_1 \boldsymbol{e}_1 \boldsymbol{e}_1^T + \lambda_2 \boldsymbol{e}_2 \boldsymbol{e}_2^T + \lambda_3 \boldsymbol{e}_3 \boldsymbol{e}_3^T, \quad (1)$$

where orientations are coded in eigenvectors $\boldsymbol{e}_1 \perp \boldsymbol{e}_2 \perp \boldsymbol{e}_3$ with their respective eigenvalues $\lambda_1 \geqslant \lambda_2 \geqslant \lambda_3 \geqslant 0$ representing pertinences.

Aligned with an input element, a tensorial field defines normal contributions in space. The contributions of every input are then accumulated for normal inference. In our method, the secondary information in resultant tensors are interpreted as indecision of normal estimation [8].

2.1 Normal tensorial field

The normal field is the most important in the accumulation method. Its trajectories define the expected curvature for surface reconstruction. We chose the vectorial and force fields with identical connecting trajectories converging to the origin.
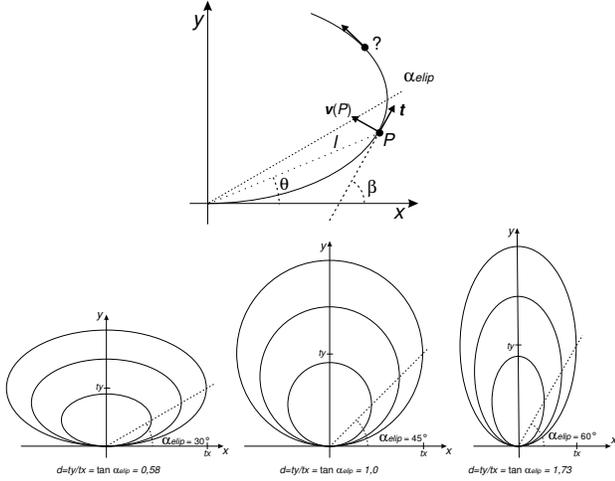
Figure 1: Ellipses with different shapes.

The trajectory curvature may be controlled by using ellipses centered in the y axis and tangent to the x axis, given by

$$\frac{x^2}{t_x^2 k^2} + \frac{(-t_y + \frac{y}{k})^2}{t_y^2} = 1 \qquad (2)$$

where t_x and t_y are constants and k define the ellipse having axis parallel to x and to y with sizes $2kt_x$ and $2kt_y$ respectively. The ellipses shape defines the connections curvature and can be easily controlled by the ratio of axis sizes

$$d = \frac{2kt_y}{2kt_x} = \frac{t_y}{t_x} \qquad (3)$$

that is the same for all ellipses of a family. Figure 1 shows some ellipse families with different values of d. The circular continuity is obtained with $d = 1$.

Given a point $P \in \mathbb{R}^2$ with polar coordinates (ρ, θ), the inclination of the line tangent to the ellipse (Eq. 2) passing by P is

$$\tan \beta = \frac{2d^2 \tan \theta}{d^2 - \tan^2 \theta}, \quad \cos \theta \neq 0 \text{ e } d \neq |\tan \theta| \qquad (4)$$

with β being the angle between this line and x axis (Fig. 1). When $|\tan \theta| = d$, the tangent line is perpendicular to the x axis ($\beta = 90°$), invalidating Eq. 4. One point cannot be connected to the origin beyond these ellipse extremes. They form the maximal connection angle α_{elip} (Fig. 1) that defines the ellipse family assigning

$$d = \tan \alpha_{elip}. \qquad (5)$$

Consider a surfel $(P, \boldsymbol{k}) \in \mathbb{R}^3 \times \mathbb{R}^3$ and the unit vectors $\boldsymbol{i} \perp \boldsymbol{j}$, all arbitrary but perpendicular to $\boldsymbol{k}$. The normal vector $\boldsymbol{k}$ defines the plan $\boldsymbol{ij}$ represented by the surfel. The point P
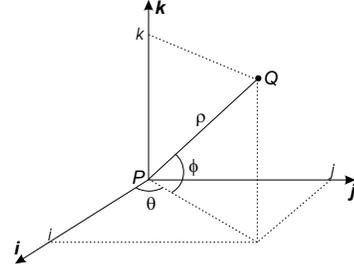

Figure 2: Spherical coordinates of a point Q in the coordinate system of a surfel $(P, \boldsymbol{k})$.

and the orthonormal base $\{\boldsymbol{i}, \boldsymbol{j}, \boldsymbol{k}\}$ form a coordinate system in $\mathbb{R}^3$ (Fig. 2). The spherical coordinates (ρ, ϕ, θ) of a point $Q \in \mathbb{R}^3$ are:

$$\rho = |PQ|, \quad \tan \phi = \frac{k}{\sqrt{i^2 + j^2}}, \quad \tan \theta = \frac{j}{i}$$

where $i = \boldsymbol{i} \cdot PQ$, $j = \boldsymbol{j} \cdot PQ$ and $k = \boldsymbol{k} \cdot PQ$ are the cartesian coordinates of Q in the system (Fig. 2). The Eq. 4 can be used to compute the angle β between the plane $\boldsymbol{ij}$ and the tangent plane to the ellipsoid passing by Q:

$$\tan \beta = \frac{2d^2 \tan \phi}{d^2 - \tan^2 \phi},$$
$$\cos \phi \neq 0, \ d = \tan \alpha_{elip} \text{ e } d \neq |\tan \phi|$$

where α_{elip} is the maximal connection angle. The 3D vectorial field for normals is defined by

$$\boldsymbol{v}_N((P, \boldsymbol{k}), Q) = (\boldsymbol{i} \cos \theta + \boldsymbol{j} \text{sen} \theta) \cos \left(\beta + \frac{\pi}{2} \right) + \boldsymbol{k} \text{sen} \left(\beta + \frac{\pi}{2} \right) \qquad (6)$$

where the addition of $\pi/2$ to β defines vectors normal to the ellipsoids.

The force gradient field should define the same trajectory of the vectorial field. Thus, the equipotential surfaces of force must be orthogonal trajectories to the ellipsoids. The farthest distance from the origin of the orthogonal trajectory passing by Q is given by

$$s((P, \boldsymbol{k}), Q) = \rho \cos \phi \left(1 + \left(2 - \frac{1}{d^2} \right) \tan^2 \phi \right)^{\frac{d^2}{2d^2 - 1}}$$

forming the attenuated scalar field

$$f_N((P, \boldsymbol{k}), Q) = e^{\frac{-s((P, \boldsymbol{k}), Q)^2}{\sigma^2}}$$

who's gradient vectors define the same trajectories of the vectorial field (Eq. 6). The normal tensorial field defining
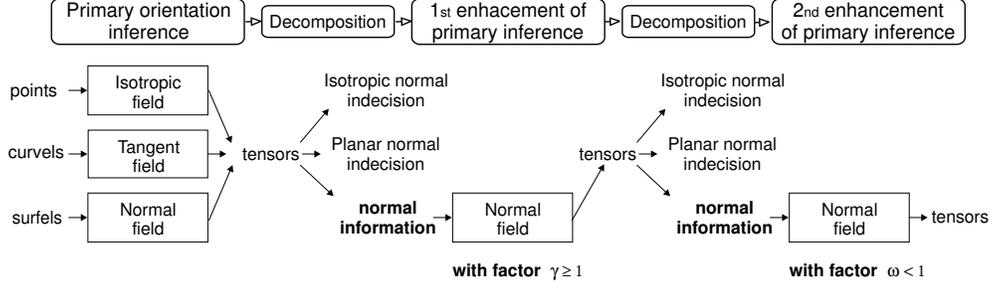
Figure 3: Orientation inference with two enhancing accumulations.

elliptical connections for a surfel $(P, \boldsymbol{k})$ in 3D is

$$\boldsymbol{C}_N((P, \boldsymbol{k}), Q) = \begin{cases} r\boldsymbol{v}\boldsymbol{v}^T, & \text{se } \phi \leqslant \alpha_{max} \\ \boldsymbol{0}, & \text{se } \phi > \alpha_{max} \end{cases},$$

$$\alpha_{max} \leqslant \alpha_{elip}, \ r = f_N((P, \boldsymbol{k}), Q), \ \boldsymbol{v} = \boldsymbol{v}_N((P, \boldsymbol{k}), Q)$$

where α_{elip} defines the maximal angle and the curvature. The α_{max} parameter can be used to define fields with smaller influence than α_{elip}.

2.2 Tangent tensorial field

A curvel $(P, \boldsymbol{t}) \in \mathbb{R}^3 \times \mathbb{R}^3$ defines a straight line that can be interpreted as an intersection of planes in space. Thus, there is only one plane passing by $(P, \boldsymbol{t})$ and a point Q having normal

$$\boldsymbol{v}_T((P, \boldsymbol{t}), Q) = \frac{\boldsymbol{w}}{|\boldsymbol{w}|}, \quad \boldsymbol{w} = \boldsymbol{t} \times PQ, \tag{7}$$

that represents the vectorial field for curvels.

The force field should be radial and stronger for points near P:

$$f_I(P, Q) = e^{\frac{-|PQ|^2}{\sigma^2}}, \tag{8}$$

where σ is the attenuation factor. The tangent tensorial field for curvels in 3D is

$$\boldsymbol{C}_T((P, \boldsymbol{t}), Q) = r\boldsymbol{v}\boldsymbol{v}^T, \ r = f_I(P, Q), \ \boldsymbol{v} = \boldsymbol{v}_T((P, \boldsymbol{t}), Q).$$

2.3 Isotropic tensorial field

A point with no associated orientation $P \in \mathbb{R}^3$ has insufficient information to induce normals directly on another point Q. Any plane passing by the straight line PQ is valid. The vectorial field defining this line

$$\boldsymbol{v}_I(P, Q) = \frac{PQ}{|PQ|}$$

should be used to code this planar indecision for normals.

Using the force equation 8, the isotropic tensorial field in 3D is

$$\boldsymbol{C}_I(P, Q) = r(\mathbf{I} - \boldsymbol{v}\boldsymbol{v}^T), \ r = f_I(P, Q), \ \boldsymbol{v} = \boldsymbol{v}_I(P, Q)$$

where $\mathbf{I}$ is the identity matrix. The plane estimated to have the normal is coded in $\boldsymbol{e}_1\boldsymbol{e}_2$ with $\boldsymbol{e}_3 = \boldsymbol{v}_I(P, Q)$ (Eq. 1). The force is coded in $\lambda_1 = \lambda_2 = f_I(P, Q)$ with $\lambda_3 = 0$.

2.4 Primary orientation inference

The primary inference is performed by the accumulation of influences of all input points. Consider an input set D composed of $n = i + j + k$ elements. To infer their orientations, every element of the total input points

$$Q = \{P_1, \cdots, P_i\} \cup \{N_1, \cdots, N_j\} \cup \{T_1, \cdots, T_k\}, \tag{9}$$

has an associated orientation tensor $\boldsymbol{T}_m \in \{\boldsymbol{T}_1, \cdots, \boldsymbol{T}_n\}$ representing the total influence of sparse data

$$\boldsymbol{T}_m = \sum_i \boldsymbol{C}_I(P_i, Q_m) + \sum_j \boldsymbol{C}_N((N_j, \boldsymbol{n}_j), Q_m) \\ + \sum_k \boldsymbol{C}_T((T_k, \boldsymbol{t}_k), Q_m)$$

where Q_m is the m-esime point of Q. Every tensor $\boldsymbol{T}_m$ contains the inferred orientation for its corresponding point Q_m from every input elements of D. This is primary information because the tangent and isotropic tensorial fields do not define smooth surfaces. Besides, noisy elements have the same weight of more precise elements.

2.5 Enhancing the primary inference

We propagate the information of normal contained in $\boldsymbol{T}_m$ using the normal tensorial field to enhance the primary inference. We argue that:

- the normal field is morphologically adapted to infer normals forming smooth surfaces and balanced pertinences;

- the use of the pertinence obtained in primary inference reduces the effect of less structured elements. We hope that noisy elements have lower pertinence;

- the information repropagation allows an extended evaluation of normal vectors.

The normal information of an orientation tensor $A = \lambda_1 e_1 e_1^T + \lambda_2 e_2 e_2^T + \lambda_3 e_3 e_3^T$ is given by functions

$$vn(A) = e_1, \qquad s(A) = \lambda_1 - \lambda_2$$

where vn is the normal vector and s is its pertinence.

A new tensor set $U_m \in \{U_1, \cdots, U_n\}$ is associated to the set of input points Q and defined by the propagation of the normal information contained in T_m:

$$U_m = \sum_{l=1}^{n} s(T_l)^\gamma \, C_N((Q_l, vn(T_l)), Q_m) \qquad (10)$$

where $(Q_l, vn(T_l))$ is the tuple composed by n input points and their estimated normals.

The factor γ is used for pertinence regularization. If $\gamma \geqslant 1$, the difference among them is amplified. Elements with low pertinence tends to have lower influence, favoring noise filtering. This may generate holes in regions with low point density. If $\gamma < 1$, the difference between pertinences is reduced, inducing an influence equalization. In presence of noise, this may disturb reconstruction processes.

For general applications, we suggest propagating normal information twice (Fig. 3). The first time, we estimate U_m with $\gamma \geqslant 1$ (Eq. 10) to filter the primary orientations. Associating the tensor set $V_m \in \{V1, \cdots, V_n\}$ to the set of input points Q, the second normal propagation is given by

$$V_m = \sum_{l=1}^{n} s(U_l)^\omega \, C_N((Q_l, vn(U_l)), Q_m) \qquad (11)$$

where $\omega < 1$ is the regularization factor. This second accumulation reduces the difference among the pertinences obtained in U_m, also reducing the filtering effect in regions with low point density.

Two accumulations were effective to enhace the normal estimation but the process may be modified. Experiments performed show that $\gamma = 1$ and $\omega = 1/2$ give good results in general applications.

3 Sparse data filtering

We assume sparse data formed by ne points structured on surfaces and nd unorganized points that were incorrectly sampled or have strong additive noise. The filtering process should be able to segment the ne pontos, labeling them as organized.

The symmetric matrices $M_i = \lambda_1 e_1 e_1^T + \lambda_2 e_2 e_2^T + \lambda_3 e_3 e_3^T$, resulted from the sparse accumulation above, give the normal pertinence

$$s(M_i) = \lambda_1 - \lambda_2$$

to each input point P_i. With this organization indicator, one may establish hypothesis to detect points structured on surfaces.

Obviously, it depends on the accumulation methods ability for retrieving consistent pertinences. Successive enhancements, as proposed in [6], infer better orientations and perform efficient sparse data filtering.

Ideally, the sparse accumulation should assign maximal pertinence to the structured points and minimal to the unorganized. The original methods of Guy, Lee [9] and the method described here tend to give greater pertinences to the organized points. This bimodal aspect of pertinence distribution enable the use of a threshold for segmenting both sets.

Given a set D with n elements and their respective simetric matrices M_i resulted from sparse accumulation, one may define a threshold l that segments the points $P_i \in$ D as follows:

- if $s(M_i) \geqslant l$, P_i is organized on a surface;

- otherwise, P_i is not organized.

The pertinence values normalized between 0 and 1 makes the empirical choose of l easier. This segmentation criterion can be applied iteratively, discarding points with very low pertinence each step. In this paper, we evaluate the ability of original and proposed methods in segmenting points in one step.

As an index of filtering accuracy, we propose one *index of points correctly classified*

$$ipc = \frac{nec}{2 \cdot ne} + \frac{ndc}{2 \cdot nd} ,$$

where nec and ndc are the number of points correctly classified among the ne structured points and the nd unorganized respectively. This index range from 0,50 to 1 in function of pertinence threshold l.

4 Experimental results

Figure 4 shows an ellipsoid and an open surface. Their high level of noise makes the filtering process more difficult.
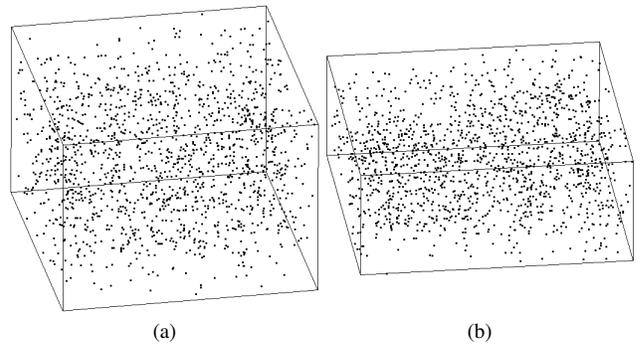

(a)   (b)

Figure 4: Sparse data for filtering evaluation. Both models are composed by 250 points with additive noise with normal distribution $\mathcal{N}(0; \, 0,02^2)$ and by 1250 incorrect points.
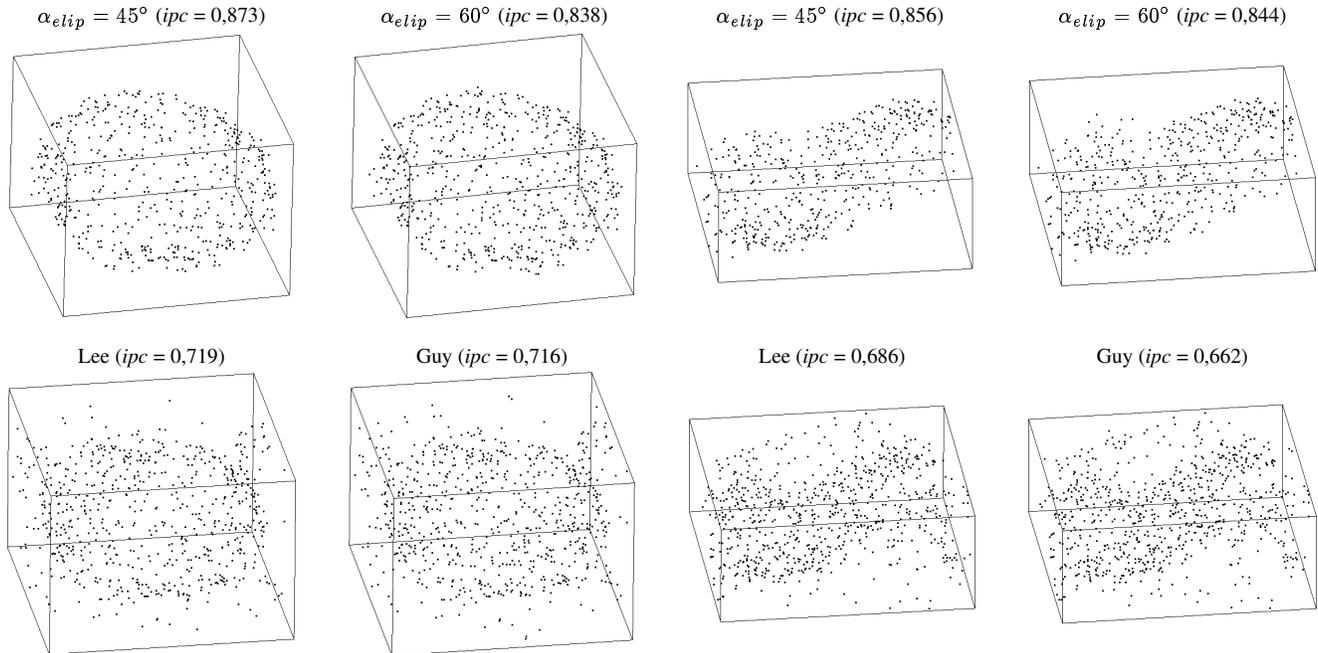
Figure 5: Filtering results of ellipsoid and open surface with *l*=0,30 and *dmax*=0,30. Shown points are classified as organized.

However, all methods obtained good results with *l*=0,30. This threshold was choosen from pertinence distributions (Fig. 6).

The filtering results for the ellipsoid and the open surface are shown in Figure 5. Visually, we can verify that the proposed accumulation method for orientation inference gives better results. Note that the number of incorrect points classified as organized is greater in the methods of Guy and Lee. The greater *ipc* values of the proposed method indicate its better performance.

We observe that the proposed method obtains pertinence distributions that favors the filtering (Fig. 6). Note that this method assigns lower pertinences to the incorrect points and greater to the structured points. Consequently, both sets are more separated than in the other methods. The standard deviations of the methods of Guy and Lee indicate a greater intersection of the pertinence distributions. It makes the filtering by threshold more difficult.

5   Conclusions

We have presented a method for sparse data filtering based on tensorial field accumulation. The accumulation process presented in [6] is used for finding precise normals and pertinence values. Filtering is performed by a simple but effective threshold segmentation of these pertinences.

Our results show a robust behavior of this filtering technique with sparse data having high noise rates. Almost all outliers have been correctly detected even with additive noise in the points sampled from objects. Our orientation enhancement step augments considerably the filtering precision. We also apply the Guy's and Lee's original methods for comparison purposes.

In [10], we propose the use of this filtering method in altimetry data to find vegetation regions. Further information about our accumulation method and its applications can be found in [6].

References

[1] Hugues Hoppe, *Surface Reconstruction from Unorganized Points*, Ph.D. thesis, University of Washington, 1994.

[2] Nina Amenta, Marshall Bern, and Manolis Kmvysselis, "A new voronoi-based surface reconstruction algorithm," in *SIGGRAPH*, 1998, pp. 415–421.

[3] M. Gopi and S. Krishman, "A fast and efficient projection-based approach for surface reconstruction," *High Performance Computer Graphics, Multimedia and Visualization*, vol. 1, no. 1, pp. 1–12, 2000.
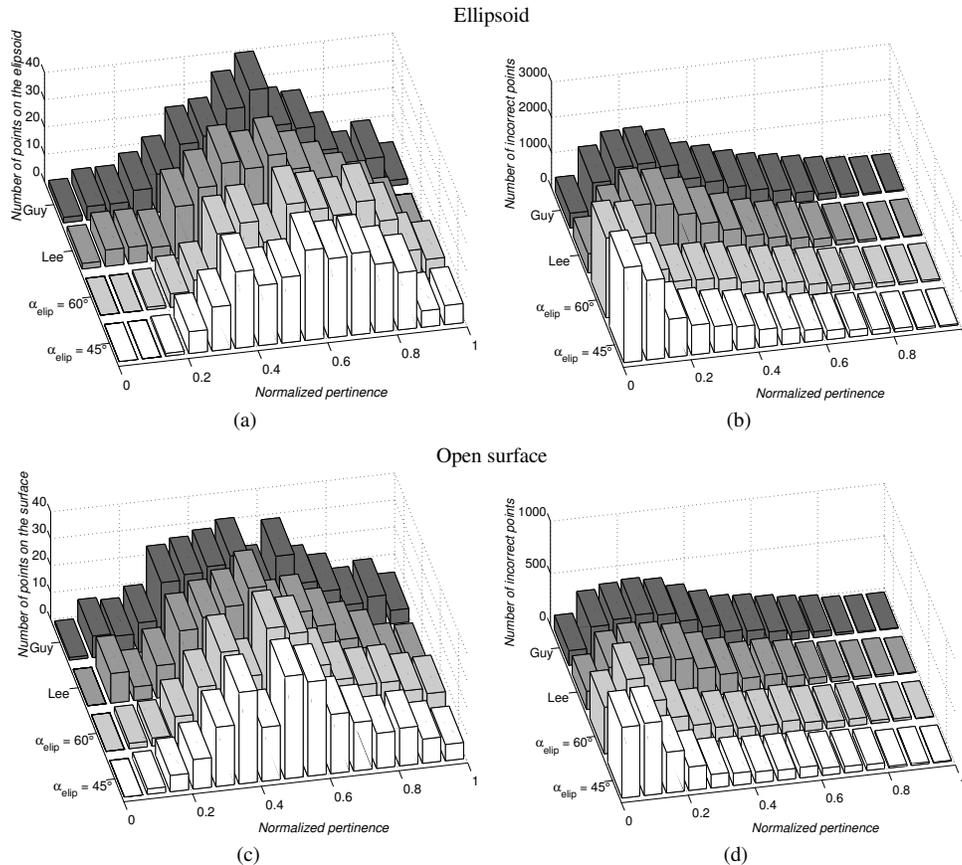
Ellipsoid

(a)

(b)

Open surface

(c)

(d)

Figure 6: Histogram of pertinences obtained in the filtering process. (a) (c) Pertinence distribution of the 250 points forming the objects (b) (d) Pertinence distribution of the 1250 incorrect points.

[4] Gideon Guy, *Inference of Multiple Curves and Surfaces from Sparse Data*, Ph.D. thesis, IRIS/University of Southern California, 1996.

[5] Gérard Medioni, Mi-Suen Lee, and Chi-Keung Tang, *A Computational Framework for Segmentation and Grouping*, Elsevier Science B.V., 1 edition, 2000.

[6] Marcelo Bernardes Vieira, *Inferência de Orientação de Dados Esparsos para Reconstrução de Superfícies*, Ph.D. thesis, Universidade Federal de Minas Gerais (UFMG) - Brazil, 2002.

[7] Hans Knutsson, "Representing local structure using tensors," in *The 6th Scandinavian Conference on Image Analysis*, Oulu, Finland, June 1989, pp. 19–22.

[8] Carl-Fredrik Westin, *A Tensor Framework for Multidimensional Signal Processing*, Ph.D. thesis, Linköping University/Sweden, 1994.

[9] Mi-Suen Lee and Gérard Medioni, "Grouping ., -, →, 0, into regions, curves, and junctions," *IEEE Compu-ter Vision and Image Understanding*, vol. 76, no. 1, pp. 54–69, Oct. 1999.

[10] Matthieu Cord, Michel Jordan, Thomas Belli, and Marcelo Bernardes Vieira, "Analyse d'images aériennes haute résolution pour la reconstruction de scènes urbaines," *Societé Française de Photogrammétrie et Télédetection*, 2002.